S.Y. Zhang, L. Yu, P. Masarati, B.W. Qiu
New General Correlations for Opening Shock Factor of Ram-Air Parachute Airdrop System
Aerospace Science and Technology, 2022, 107844 (8 pages)
doi:10.1016/j.ast.2022.107844

New general correlations for opening shock factor of ram-air parachute airdrop system

SiYu ZHANG[a, b], Li YU[a,*], Pierangelo MASARATI[c], BoWen QIU[a]

a. Key Laboratory of Aircraft Environment Control and Life Support, MIIT, Nanjing University of Aeronautics and Astronautics, Nanjing 210016, China

b. Visiting Ph.D. candidate at Department of Aerospace Science and Technology, Politecnico di Milano, 20156 Milan, Italy

c. Department of Aerospace Science and Technology, Politecnico di Milano, 20156 Milan, Italy

Abstract: The attainability of the opening process directly determines the success of a ram-air parachute airdrop system. The opening shock is the most concerned parameter for designers. Focusing on the parachute opening process, the peak load is evaluated using the opening shock factor, which is obtained using the dynamic model and the Momentum Impulse theory. Comparisons with airdrop test results show that the two methods can accurately predict the peak load. In the similarity analysis of parachutes, the criteria for flexibility, elasticity, and air permeability are summarized, and the dimensionless numbers affecting the opening shock are identified as the mass ratio, the Froude number, and the Strouhal number. The frame design of the ram-air parachute airdrop system is completed, and a database of opening shock factors including airdrop test data and numerical results is established. New general correlations for the opening shock factor are presented for vertical and horizontal opening utilizing the Levenberg-Marquardt method for regression analysis, with R^2 of 0.9935 and 0.9880, and MAPE of 2.64% and 9.8%, respectively. The new correlations can quickly and accurately predict the opening shock for ram-air parachute airdrop systems.

Keyword: Ram-air parachute; opening shock factor; peak load; correlation; dynamic model; Momentum Impulse theory

1. Introduction

Compared with traditional round parachutes, the ram-air parachute with a high lift-drag ratio is the only viable parafoil solution in practical applications [1-4], owing to extraordinary gliding performance and manoeuvrability. It has become the focus of various researchers worldwide in recent years.

From a designer's point of view, the attainability of the opening process directly determines the success of a ram-air parachute airdrop system. To obtain high gliding ratios and ideal aerodynamic shape, the canopy is usually manufactured of fabrics with ultra-low air permeability. The configuration of the suspension lines is also different from that of round parachutes. In addition to the suspension lines at the skirt, there are also several rows of different lengths connecting the fins, resulting in a shorter opening time. However, a quick opening may produce a larger shock, which is more likely to cause the canopy damage and opening failure. According to incomplete statistics, the probability of incomplete opening of ram-air

Corresponding author.
E-mail address: yuli_happy@163.com (L. Yu)

parachutes is as high as 3%, which is far higher than that of conventional round parachutes. On the other hand, with the increase of airdrop payload, the canopy areas expand, leading to an increase in opening shock and the probability of canopy damage. The peak load directly affects the safety of the airdrop system, which is usually evaluated by the opening shock factor. Therefore, its prediction is the most prominent to ensure the feasibility of the airdrop mission. Currently, the opening load is mainly acquired through dynamic calculations or airdrop tests.

A few investigations are available on the calculation of ram-air parachute opening dynamics, whereas many existing studies focus on round parachutes. Garrard [5] proposed a piecewise dynamic method for the opening process, divided into expanding and inflating stages. The opening shock can be gained based obtained from the flight mechanics equations and the time-varying aerodynamic characteristics without considering the added mass. Li [6] presented a two-dimensional opening model completely independent of experimental data or empirical values and established the canopy radial equation of motion, assuming that the ram-air parachute system is a two-particle-elastic rod model to obtain the opening shock. Based on the physical state during the opening process, Potvin's team [7] proposed an opening dynamics method for slider-reefed ram-air parachutes to predict the maximum deceleration and inflation time, which divides the opening process into three stages: centre cell pressurization, outboard cells pressurization and expansion, slider-descent and canopy expansion. Potvin's team also suggested a semi-empirical universal method [8, 9] based on the momentum theorem, which can quickly evaluate the opening shock factor. In recent years, some scholars obtain opening load by adopting coupling dynamics methods [10], which are more complicated and are more used to obtain the flow field information. Because of the structural complexity of ram-air parachutes, it is more difficult to simulate the opening process with this method. Zhang [11] achieved the coupling dynamics solution of ram-air parachute with ALE method at a high cost of calculation.

The experiments for ram-air parachute opening shock are mainly carried out using airdrop tests, which are classified into tower, balloon, and aircraft. Among them, the operating conditions such as velocity and altitude can be controlled to achieve test repeatability in tower-drop tests. However, large-area ram-air parachute tests are limited by the height of the tower. China Aerospace Science and Technology Corporation (CASC) [12] has launched more than 40 tower drop tests to verify the coordination of the opening process. Besides, balloons [13] can be used for fixed-point airdrop tests at low cost and convenient implementation. However, due to the influence of weather and the unavailability of the initial velocity, it is usually used for light-weight and low-altitude airdrops. The United States conducted high-altitude balloon tests on the HAHO Parafoil System [14], but all tests encountered partial or total failure due to delayed or failed inflation. In practice, aircraft airdrop tests are the most direct of effective method despite of high cost and poor repeatability. Most ram-air parachute airdrop tests from aircraft are performed in the USA, such as the army Natick soldier centre [15, 16] and Parks University [17]. NASA also conducted several airdrop tests on the X-38 return system [18, 19] equipped with a large ram-air parachute, which successfully demonstrated deploying, repeatability of opening, and precise and soft landing. Besides, CASC [20] implemented a controllable recovery of a 4000kg rocket booster using China's largest ram-air parachute in 2021. Zeng [21] proposed an analysis method for opening load based on the measured acceleration and attitude parameters, which is also completely dependent on the airdrop test.

As mentioned above, most existing dynamic calculations are based on the Newton-Euler method, the solution of which requires programming and cannot be got quickly. And airdrop tests have the disadvantages of a long cycle, high cost, great risk, and many external influence factors. Especially for large-area ram-air parachutes, the implementation of their airdrop tests is more difficult. Therefore, there is an urgent need for a dimensionless general method that can quickly and accurately predict the opening shock factor as it can reduce cost caused by over-design or avoid risk caused by under-design. Firstly, it is necessary to analyse the similarity of ram-air parachute opening process and derive the corresponding dimensionless numbers for general correlations. Existing similarity researches mainly focus on round parachutes [22, 23]. French [24] handled the similarity study of the opening shock based on the dynamic method and wind tunnel tests, then evaluated the qualitative influence of the Euler and Froude numbers and the mass ratio. Lingard [25] presented a semi-empirical theory of opening shock varying with time and discovered that the peak load mainly depends on the mass ratio and the Froude number. Lee [26] studied the opening characteristics of C9 parachutes with full-size, 1/2 scaled, and 1/4 scaled models through experiments and determined that the mass ratio, the Froude number, and the stiffness index are the three independent dimensionless numbers affecting the opening process. Lately, Potvin [27] took C9 parachute as the research object, focused on extrapolating the opening performance of large-scale parachutes using smaller-sized parachutes, and discussed the relationship between the non-dimensional metrics of peak drag and several dimensionless numbers.

In the similarity surveys, the model and prototype parachutes are usually composed of the same flexible fabrics but their overall flexibility is radically different. Heinkich and Hektner [28] initially proposed the stiffness index to measure the flexibility of parachutes according to their structural characteristics. Niemi [29, 30] modified the original stiffness index by eliminating the Poisson ratio and introducing the dynamic pressure.

Most investigations of the similarity studies for ram-air parachutes are conducted by Potvin's team. Potvin [31] showed that the maximum deceleration depends on a dimensionless constant, i.e., a configuration scaling number determined by packing style, slider and suspension line lengths, etc. In reference [9], the author illustrated the correlation for maximum deceleration with this dimensionless constant. Additionally, Potvin [32, 33] elaborated the similarity laws for the influence of height and payload on ram-air parachutes in the opening process based on the three-stage model and found that the altitude- and weight- scaling properties of ram-air parachutes show trends very similar to those of round ones.

Aiming at the opening process, new general correlations are presented to make it possible to get the opening shock factor of the ram-air parachute airdrop system quickly and accurately. Moreover, the peak load takes the average value of the results calculated by different methods to avoid the one-way deviation caused by a certain method. In the regression analysis, a large number of airdrop data are introduced to increase the reliability of the overall data and ensure the accuracy of the correlations. Based on the similarity criteria summarized in this paper, the opening performance of large-area parachutes can be estimated by using small parachutes as models, which avoids the problem that large-area parachutes are difficult to be tested. The paper is organised as follows. The numerical investigation of the peak load is implemented in Section 2 and validated in Section 3. The dimensional analysis of the opening process for ram-air parachutes is described in Section 4. The new general correlations for the opening shock factor are presented in Section 5. Concluding remarks are given in Section 6.

2. Numerical investigation of peak load

2.1 Dynamic model of the opening process

The dynamic model of the opening process of a ram-air parachute airdrop system is established in the flight-path axis system without considering the additional mass and the relative position between parachute and payload in the opening process:

$$\begin{cases} m_s \dfrac{dv}{dt} = -m_s g \sin\theta_{gj} + F_k - \dfrac{1}{2}\rho v^2 C_{D,s} A_0 \\ m_w \dfrac{dv}{dt} = -m_w g \sin\theta_{gj} - F_k - \dfrac{1}{2}\rho v^2 C_{D,w} A_w \\ (m_s + m_w) v \dfrac{d\theta_{gj}}{dt} = -(m_s + m_w) g \cos\theta_{gj} + \dfrac{1}{2}\rho v^2 C_{L,s} A_0 \end{cases} \tag{1}$$

where, t, m_s, m_w, $A_0 = bc$, $C_{D,w}A_w$, ρ, g, v, θ_{gj}, F_k, $C_{D,w}$, $C_{D,s}$, and $C_{L,s}$ respectively represent time, parachute mass, payload mass, parachute nominal area, payload drag area, air density, gravity acceleration, velocity, flight path angle, opening shock, the drag coefficient of the payload, and drag and lift coefficients of the ram-air parachute; b is the span, c is the chord. The variation of aerodynamic characteristics with time in the opening process of the ram-air parachute is shown in Figure 1.

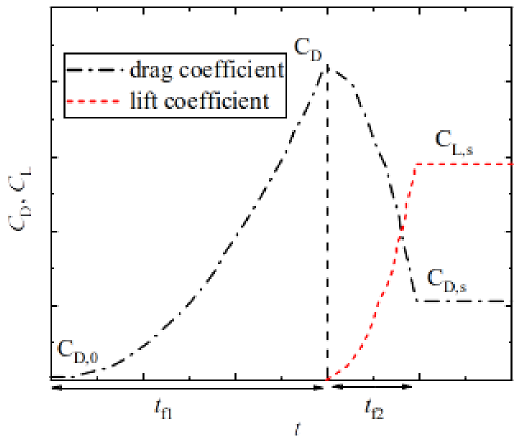

Figure 1 Variation of aerodynamic characteristics with time in the opening process of the ram-air parachute.

As shown in the figure, $C_{D,0}$ and C_D are the drag coefficients of the parachute at the beginning and end of the first opening stage, respectively. In the first opening stage, the wing gradually expands like a rectangular parachute without inflation, and the drag coefficient increases continuously without any lift generation. It is found in many experiments and papers that $C_D = 1.0$ is a universality parameter for ram-air parachutes in the first opening stage. In the second stage, the cells inflate until full inflation and the parachute generates lift while the drag reduces. $C_{L,s}$ and $C_{D,s}$ are the lift coefficient and drag coefficient after stabilization respectively, which of various parachutes are different, but there is no effect on the peak load. $t_{f1} = \lambda_1 D_0 / v_c$ and $t_{f2} = \lambda_2 D_0 / v_c$ respectively represent the filling time of the two stages. $D_0 = \sqrt{4A_0/\pi}$ is the nominal diameter, v_c is the initial velocity, and λ_1, λ_2 are the correction coefficients. In this paper, $\lambda_1 = 18$ and $\lambda_2 = 2.5$ are considered for the slider-reefed ram-air parachutes according to experimental results.

2.2 Prediction based on Momentum-Impulse theory

As opposed to the full ballistic calculation of Section 2.1, the prediction method in this section only focuses on the peak load $F_{\mathrm{k\,max}}$. The analysis of the initial opening stage shows that the drag coefficient is much greater than that during gliding flight, the lift can be almost ignored, and the peak load also appears in this stage.

It is assumed that drag is always tangent to the flight trajectory in the opening process, as shown in Figure 2, where the subscripts c and z respectively represent the initial and final time of the opening. Based on the Momentum-Impulse theory [34], the following equation is established along the flight trajectory for the opening process:

$$mv_z - mv_c = \int_{t_c}^{t_z} F_{\mathrm{k}}(t)\,dt + \int_{t_c}^{t_z} mg\sin\theta_{\mathrm{gj}}(t)\,dt \tag{2}$$

where, m is the mass of ram-air parachute-payload system.

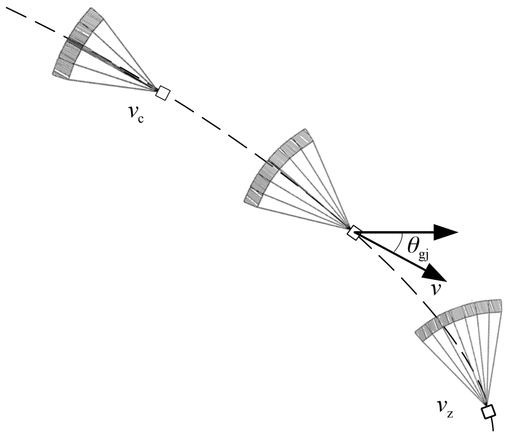

Figure 2 Trajectory of ram-air parachute in opening process.

The dimensionless opening shock factor is defined as:

$$C_{\mathrm{k}} = \frac{F_{\mathrm{k\,max}}}{\frac{1}{2}\rho v_c^2 (C_{\mathrm{D}} A_0)} \tag{3}$$

Equation (3) is replaced in equation (2), yielding the following deformation:

$$mv_z - mv_c = -C_{\mathrm{k}}\frac{1}{2}\rho v_c^2 (C_{\mathrm{D}} A_0)(t_z - t_c)\int_{t_c}^{t_z} \frac{\left|F_{\mathrm{k}}(t)\right|}{F_{\mathrm{k\,max}}(t_z - t_c)}dt + \int_{t_c}^{t_z} mg\sin\theta_{\mathrm{gj}}(t)\,dt \tag{4}$$

The aerodynamic drag integral $I^F = \int_{t_c}^{t_z} \frac{\left|F_{\mathrm{k}}(t)\right|}{F_{\mathrm{k\,max}}(t_z - t_c)}dt$ contains information on the drag force with respect to the nominal area. In addition, it reduces the sensitivity to actual drag fluctuations, reducing the influence of local errors on the overall momentum of the system.

Finally, the desired opening shock factor is obtained as:

$$C_k = 2\left(\frac{m}{\rho(C_D A_0)^{1.5}}\right)\left(\frac{(C_D A_0)^{0.5}}{v_c(t_z - t_c)I^F}\right)\frac{-(v_z - v_c) + \int_{t_c}^{t_z} g\sin\theta_{gj}(t)\,dt}{v_c} \tag{5}$$

In the third and last contribution, the first half represents the momentum change of the ram-air parachute-payload system at unit mass and unit velocity, whereas the second half represents the momentum due to gravity. Considering two extreme cases, when the parachute opening process is horizontal, θ_{gj} remains 0°, whereas when the opening process is vertical, θ_{gj} remains 90 °.

The flight velocity at the end of the opening process is obtained through the dynamic model of Section 2.1, which differs from Potvin's approximate solution using steady descent velocity. Compared with the final time of the opening process, the steady descent phase occurs later, and loss of momentum still takes place in this process, which will lead to the problem of overestimating the value of the opening shock factor.

In actual opening tests, the data of identical ram-air parachutes under identical airdrop conditions are often inconsistent. This is due to the non-deterministic behaviour of the flexible canopy. The insensitivity of the aerodynamic drag integral to the local fluctuation of the opening shock curve can effectively mitigate this problem. According to the collection and analysis of substantial test data, it is found that the range of I^F remains between 0.4–0.5. In this paper, I^F =0.5.

3. Verification and validation

The airdrop test data of the MC-4 [5] and Strato cloud parachute [35] are used to verify the calculation of reefed and unreefed ram-air parachutes respectively. The calculation conditions and structural parameters of ram-air parachutes are shown in Table 1.

Table 1
Calculation conditions and structural parameters of ram-air parachutes.

Parafoil	Span	Chord	θ_{gj}	Height	Velocity	Mass
MC-4 (Reefed)	8.69m	3.96m	80°	7500m	76.2m/s	163.3kg
Strato Cloud (Unreefed)	5.84m	3.07m	90°	150m	37.8m/s	72.5kg

Note: the flight path angle of the MC-4 parachute is set to 90° in calculation based momentum impulse theory.

The opening shock curve obtained by the dynamic model is compared with airdrop tests, as shown in Figure 3. The initial time is recorded as 0. The comparison of the opening shock between the values calculated by two methods and airdrop test results is shown in Table 2. In these two cases, t_{f1} =1.56s and t_{f2} =0.22s for the reefed ram-air parachute, t_{f1} =0.30s and t_{f2} =0.20s for the unreefed ram-air parachute.

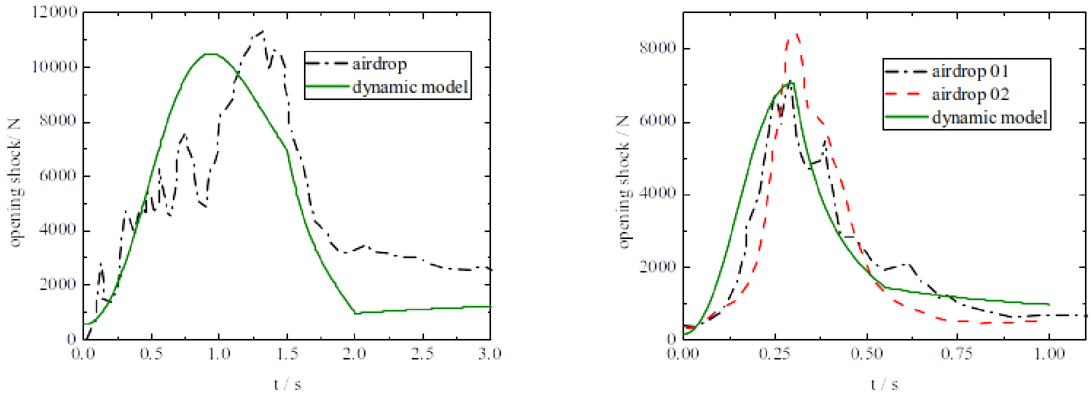

(a) MC-4 (b) Strato Cloud

Figure 3 Variation of opening shock.

Table 2

Comparison of peak load between calculations and test results.

Parafoil	Airdrop test	Dynamic model		Momentum-Impulse theory	
		Peak load	Error	Peak load	Error
MC-4 (Reefed)	11393 N	10503 N	7.81%	12063 N	5.88%
Strato Cloud (Unreefed)	7803 N	6958 N	10.83%	7243 N	7.18%

Note: the peak load of the Strato cloud parachute in the two airdrop tests is 7191 N and 8415 N, respectively, and the average value of the test load, 7803 N, is taken as reference for the Momentum-Impulse theory

Figure 3 and Table 2 indicate that the variation of parachute opening load calculated by the dynamic model is consistent with the trend of the airdrop tests. Besides, the peak load errors calculated by two methods are all within the error requirement scope of 20% of the flexible parachute opening analysis. Hence, the calculation models can accurately obtain the peak load during the opening process.

4. Dimensional analysis of the opening process

4.1 Criteria for flexibility, elasticity and air permeability

The traditional similarity laws should be satisfied first in the similarity analysis of the opening process. Secondly, since a ram-air parachute's characteristics such as fabric elasticity, flexibility and air permeability radically differ from those of a rigid body, the criteria for these should also be considered before the dimensional analysis of the opening shock.

The main parameters affecting structural elasticity are: the nominal diameter D_0, the elastic modulus of the canopy E_c, the elastic modulus of the suspension lines E_s, the air density ρ, and the opening velocity V_c. According to the dimensional consistency principle of the Buckingham π theorem[36], the Cauchy numbers representing the ratio of inertial to elastic forces are obtained:

$$Ca_c = \frac{\rho v_c^{\ 2}}{E_c} \tag{6}$$

$$Ca_s = \frac{\rho v_c^{\ 2}}{E_s} \tag{7}$$

Additionally, severe deformation occurs in the opening process due to the flexibility of materials. The flexibility is evaluated by the stiffness index [28]:

$$\eta = \frac{D_{\max}}{D_0}\frac{m_s}{A_0 m_{un}} \tag{8}$$

where, $D_{\max}$ is the maximum width of the suspended canopy, whereas m_{un} is the fabric weight per unit area.

The porosity of ram-air parachutes is composed of geometric and fabric porosity. Among them, the geometric porosity is determined by the opening area, thus the similarity of geometric porosity between prototype and model can be guaranteed by their geometric similarity. Concerning fabric porosity, although the canopy is mainly composed of fabric with low air permeability, its influence on aerodynamic performance cannot be overlooked. In some cases, the fabric porosity changes the aerodynamic coefficients by 50% [37]. The fabric porosity is usually expressed by the dimensionless effective permeability:

$$W_y = \frac{v_q}{v} \tag{9}$$

where, v_q is the air permeability of the fabric, which can be gained by Zhang model [38]:

$$v_q = \frac{-\frac{25\mu}{6\delta\varepsilon^3} + \sqrt{\frac{625\mu^2}{36\delta^2\varepsilon^6} + \left(\frac{7}{12\varepsilon^3}+1\right)\rho^2 v^2}}{\rho\left(\frac{7}{12\varepsilon^3}+1\right)} \tag{10}$$

where, μ is dynamic viscosity of air, δ is the thickness of canopy, and ε is the inherent property of fabric, which is the ratio of void volume to total volume.

4.2 Dimensionless numbers affecting the peak load

In the actual opening process, there are two modes: free fall and static line, respectively corresponding to the vertical opening and approximate horizontal opening. Accordingly, when the initial angle is determined, the main parameters affecting the peak load in the opening process according to the numerical model are shown in Table 3. The selected basic dimensions are the length L, the quality M and the time T .

Table 3

Main parameters affecting the peak load.

Symbol	Definition	dimension

F_{kmax}	Peak load	MLT^{-2}
m	Mass of system	M
ρ	Air density	ML^{-3}
v_c	Initial velocity	LT^{-1}
g	Gravity	LT^{-2}
D_0	Nominal diameter	L
t	Inflation time	T

Considering ρ, D_0 and v_c as the basic variables and according to the dimensional consistency principle of Buckinghamπ theorem, the dimensionless numbers can be obtained as follows:

$$\pi_1 = \frac{F_{\text{kmax}}}{\rho v_c^2 D_0^{\ 2}} \tag{11}$$

$$\pi_2 = \frac{m}{\rho D_0^{\ 3}} \tag{12}$$

$$\pi_3 = \frac{g D_0}{v_c^2} \tag{13}$$

$$\pi_4 = \frac{v_c t}{D_0} \tag{14}$$

The following dimensionless numbers with physical meaning are obtained through further manipulation:

$$C_{\text{k}} = \frac{F_{\text{kmax}}}{\frac{1}{2}\rho v_c^2 (C_{\text{D}} A_0)} \tag{15}$$

$$Rm = \frac{m}{\rho (C_{\text{D}} A_0)^{1.5}} \tag{16}$$

$$Fr = \frac{v_c^2}{g D_0} \tag{17}$$

$$Sr = \frac{D_0}{v_c t} \tag{18}$$

where, Rm is the mass ratio representing the ratio of the payload to the mass of the air driven by the parachute during flight, F_r is the Froude number, representing the proportional relationship between the inertia force and gravity, Sr is the Strouhal number, associated with the time-dependence of the process.

The definition of mass ratio is not uniform in the literatures. In early researches, Johari [39] and

Berndt [40] defined the parachute mass ratio as $Rm = \frac{m}{\rho D_0^3}$. After recognizing the influence of aerodynamic characteristics, Lingard [25] and Wolf [41] revised the mass ratio as $Rm = \frac{m}{\rho C_D D_0^3}$. In subsequent development, Potvin [42] defined it as $Rm = \frac{\rho (C_D A)_{sd}^{1.5}}{m}$, the subscript sd representing the projected area during steady descent. In this paper, equation (16) is uniformly used as the definition of mass ratio.

According to the Buckingham theorem in dimensional analysis, the function between the opening shock factor and the dimensionless numbers should be as the following form:

$$C_k = f(Rm, Fr, Sr) \tag{19}$$

5. General correlations for the opening shock factor

5.1 Frame design of ram-air parachute airdrop system

In order to make the correlations for the opening shock factor more widely used, a ram-air parachute airdrop system with a payload range of 80-20,000 kg is selected as the research object. At present, only the Joint Precision Airdrop System (JPADS) [43, 44] can deliver different payloads from Extra-Light to Heavy, namely, from 200 lb to 60,000 lb. Therefore, the ram-air parachute system is designed with a reasonable wing loading referring to the JPADS. The relationship between the nominal area and the payload of the JPADS is shown in Figure 4.

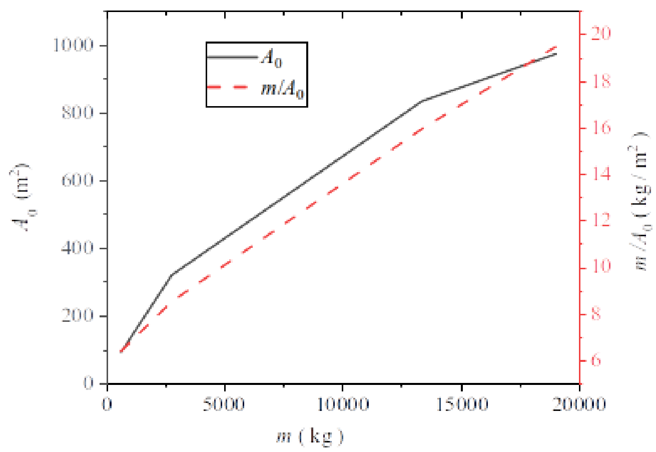

Figure 4 Variation of area and wing loading with mass in JPADS system.

Figure 4 suggests that with the increase of the payload, the canopy area increases as well. Actually, the canopy area cannot be increased excessively, so the wing loading (i.e., the payload per unit area) also grows approximately linearly with the mass. This is because the larger the parachute area, the greater the parachute opening shock, and the more likely to result in the failure of parachutes. Besides, it is very difficult to manufacture large-area parachutes

In the initial opening process, the air density of 1.0 kg/m^3 is considered. Accordingly, under the assumption that the wing loading varies linearly with the mass, the wing loading and mass ratio of the designed airdrop system change with the mass as shown in Figure 5. It shows that the mass ratio decreases sharply at first, and then slowly increases with the increase of mass. Besides, the mass ratio of the light ram-air parachute airdrop system is larger than that of the heavy airdrop system. The range of mass ratio is $0.449 \le R_m \le 1.814$, and the minimum value is 0.45 at 4290 kg.

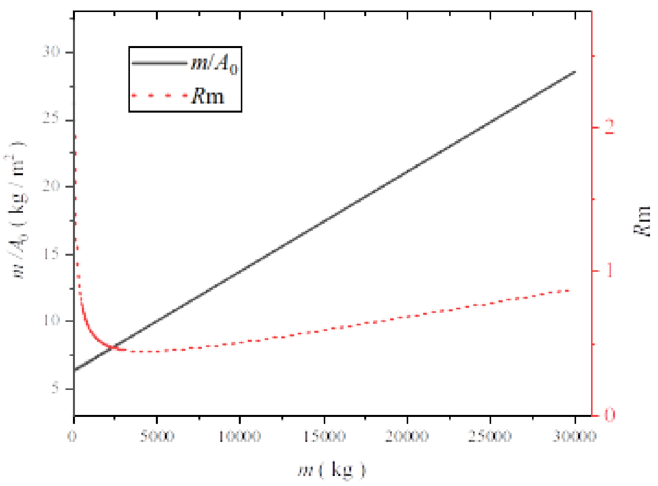

Figure 5 Variation of wing loading and mass ratio with mass.

5.2 Regression method

To predict the peak load, the correlations for the opening shock factor are studied in this section. The average value obtained by the opening dynamic model and Momentum-Impulse theory is taken as the opening shock factor, which avoids the error and the cumulative deviation caused by a certain numerical simulation technology. Moreover, 420 data based on airdrop tests[5, 6, 9, 17, 31, 35, 45] are combined to form a database of 1877 opening shock factors, which not only increases the authenticity and credibility of the overall data but also avoids the huge cost and risk caused by using only an experimental method.

The multiple nonlinear regression analysis of the correlation is carried out according to the database. The objective function is rewritten as follows:

$$C_k = f(Rm, Fr, Sr) = f(\boldsymbol{R}, \beta) \tag{20}$$

where, $\boldsymbol{R} = (Rm, Fr, Sr)$ is the independent variable and $\beta = (a_1, a_2, \cdots, a_m)$ is the undetermined coefficient. The next goal is to find β to minimize the residual sum of squares $\chi(\beta)$ between the regression values and the original values:

$$\chi(\beta) = \sum_{i=1}^{n} \left(C_{k,i} - \hat{C}_{k,i} \right)^2 = \sum_{i=1}^{n} \left(C_{k,i} - f(\boldsymbol{R}_i, \beta) \right)^2 \tag{21}$$

The Levenberg-Marquardt method [46] is utilized to deal with the nonlinear least squares fitting problem. Similar to other optimization methods, given an initial parameter β firstly, the parameter vector β is replaced by a new estimation $\beta + h$ in each iteration step; $h = (h_1, h_2, \cdots, h_m)$ is the increment.

The formula of $f(R_i, \beta + h)$ is expanded in Taylor series:

$$f(R_i, \beta + h) = f(R_i, \beta) + J_i h + O(h^T h) \tag{22}$$

where, $J_i = \frac{\partial f(R_i, \beta)}{\partial \beta}$ is the Jacobian matrix. Bringing the above equation into equation (21) and omitting the infinitesimal term yields

$$\chi(\beta + h) \approx \sum_{i=1}^{n} \left(C_{k,i} - f(R_i, \beta) - J_i h\right)^2 \tag{23}$$

The vector form of the above formula is written as:

$$\chi(\beta + h) \approx \left\| C_k - f(\beta) - Jh \right\|^2 \tag{24}$$

where, $C_k = (C_{k,1}, C_{k,2}, \cdots, C_{k,n})$, $f(\beta) = [f(R_1, \beta), f(R_2, \beta) \cdots, f(R_n, \beta)]$. Setting the derivative with respect to h equal to zero gives

$$\left[J^T J\right] h = J^T \left[C_k - f(\beta)\right] \tag{25}$$

In the least square method, the Hessian matrix $J^T J$ must be invertible. A regularization factor [47] is introduced to avoid singularities of the Hessian matrix:

$$\left[J^T J + \lambda E\right] h = J^T \left[C_k - f(\beta)\right] \tag{26}$$

where, E is the identity matrix and λ is the non-negative damping parameter, which is continuously adjusted with the iterative calculation. In addition, replacing E with the diagonal of the Hessian matrix, i.e., $diag(J^T J)$, gives:

$$\left[J^T J + \lambda \cdot diag(J^T J)\right] h = J^T \left[C_k - f(\beta)\right] \tag{27}$$

The coefficient of determination (R^2) and mean absolute percentage error (MAPE) are selected as the criteria to judge the regression analysis of correlations. The coefficient of determination indicates the fitting degree of the regression equation, which is defined as:

$$R^2 = \frac{\sum_{i=1}^{n}\left(C_{k,i} - \overline{C_{k,i}}\right)^2}{\sum_{i=1}^{n}\left(C_{k,i} - \overline{C_{k,i}}\right)^2} = 1 - \frac{\sum_{i=1}^{n}\left(C_{k,i} - C_{k,i}\right)^2}{\sum_{i=1}^{n}\left(C_{k,i} - \overline{C_{k,i}}\right)^2} \tag{28}$$

where C_k is a datum in the database, $\hat{C}_k$ is the prediction calculated by the correlation, $\overline{C_k}$ is the average value in the database, n is the number of data.

The MAPE is a measure of prediction accuracy in statistics, which is defined as:

$$\text{MAPE} = \frac{100\%}{n} \sum_{i=1}^{n} \left| \frac{C_{k,i} - \hat{C}_{k,i}}{C_{k,i}} \right| \tag{29}$$

5.3 General correlation

The new general correlations of two extreme opening conditions are implemented respectively in this section. One is the horizontal opening, with the subscript *h*, and the other is the vertical opening, with the subscript *v*. The value range of opening shock factor at any angle is $C_{kh} \le C_k \le C_{kv}$.

On the one hand, for the vertical database (C_{kv}) composed of 1148 opening shock factors, the general correlation obtained based on MATLAB is as follows

$$C_{kv} = 0.0315\left(Rm + 0.0454\right)\left(\arctan\left(\frac{Fr}{27.7875}\right)^{-0.8002}\right)\left(\ln\left(Sr\right) + 8.2838\right) \tag{30}$$

The presented correlation for the vertical opening process has the R^2 of 0.9935 and the MAPE of 3.45%. Figure 6 shows the comparison of predictions with the database in the vertical opening process. It suggests that the predictions of the new correlation for the vertical opening process are in good agreement with the database, except that only a few data are without the error range (20%).

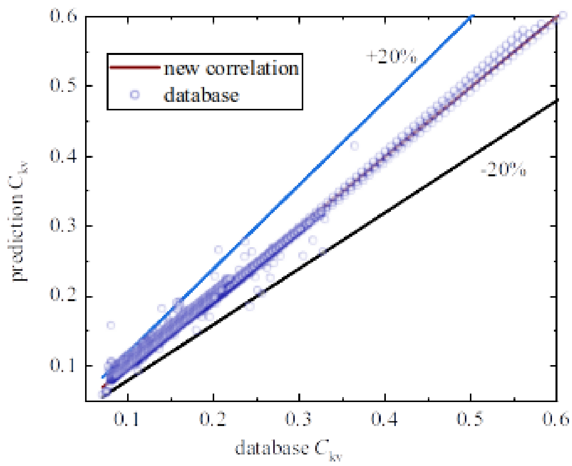

Figure 6 The comparison of predictions with the database in the vertical opening process.

On the other hand, for the horizontal database (C_{kh}) composed of 729 opening shock factors, the general correlation obtained using the L-M method is as follows:

$$C_{kh} = 0.0719\left(Rm + 0.2431\right)\left(\ln\left(Sr\right) + 4.4227\right) \tag{31}$$

The presented correlation for the horizontal opening process has the R^2 of 0.9880 and the MAPE of 2.64%. Figure 7 shows the comparison of predictions with the database in the horizontal opening process. It reveals that the predictions of new correlation for the horizontal parachute opening are well consistent with the database and all data are within the error range (20%).

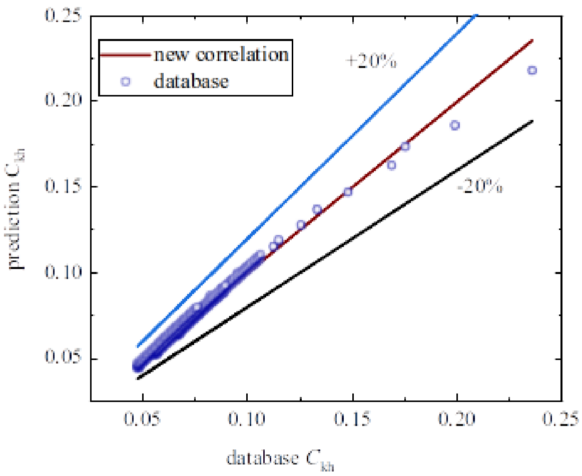

Figure 7 The comparison of predictions with the database in the horizontal opening process.

Based on the above discussion, the range of opening shock factor at any angle is $C_{kh} \le C_k \le C_{kv}$, and the peak load in the opening process is further obtained according to $F_{k\max} = \frac{1}{2} C_k \rho v_c^2 (C_D A_0)$.

6. Conclusions

This paper solves the problem that it is difficult to predict the opening load of the ram-air parachute airdrop system quickly and accurately. A prediction method for peak load adopts the opening dynamic model and Momentum Impulse theory to avoid the one-way deviation caused by a certain approach. The dimensional analysis of the parameters affecting the peak load is developed and new general correlations for the opening shock factor are proposed. In general, some conclusions can be drawn:

1. The unsteady variation of the opening shock during the whole flight trajectory in the opening process is obtained using the dynamic model. Based on the Momentum Impulse theory, a prediction for the opening shock factor is presented by adopting the dynamic model to modify the final velocity in the opening phase. Comparisons with the airdrop test results show that the errors of the peak load calculated by the two methods are within the error requirement scope of 20% of the flexible parachute opening analysis. Thus, the numerical approaches in this paper can accurately predict the peak load in the opening process.

2. Similarity criteria for flexibility, elasticity and air permeability of parachutes are summarized according to the dimensional analysis. The dimensionless numbers affecting the opening shock are proposed, which are the mass ratio, the Froude number, and the Strouhal number.

3. The area and wing loading of the ram-air parachute airdrop system in the wide range of 80-20000 kg are designed. A database of opening shock factors containing 420 data of airdrop test results and several calculations obtained by the dynamic model and the Momentum Impulse theory is constructed, including

1148 vertical data and 729 horizontal data, with a mass ratio range of $0.449 \le R_m \le 1.814$.

4. The Levenberg-Marquardt method is used for multivariate nonlinear least-squares regression analysis, and new general correlations are proposed for vertical and horizontal parachute opening, with R^2 of 0.9935, 0.9880 and MAPE of 2.64%, 9.8% respectively.

Conflict of interest statement

There is no conflict of interest for this manuscript.

Acknowledgements

The first authors acknowledge the financial supported by China Scholarship Council.

Funding

This work was supported by Chinese National Natural Science Foundation (Grant No. 11972192), Interdisciplinary Innovation Foundation for Graduates, NUAA (Grant No. KXKCXJJ202003) and the Priority Academic Program Development of Jiangsu Higher Education Institutions.

References

[1] H. Sun, S. Luo, Q. Sun, Z. Chen, W. Wu, J. Tao, Trajectory optimization for parafoil delivery system considering complicated dynamic constraints in high-order model, Aerospace Science and Technology, 98 (2020) 105631.

[2] R. Benney, J. McGrath, J. McHugh, G. Noetscher, S. Tavan, S. Patel, DOD JPADS Programs Overview and Nato Activities, AIAA Paper 2007-2576, 2007.

[3] M. Ghoreyshi, K. Bergeron, A. Jirásek, J. Seidel, A.J. Lofthouse, R.M. Cummings, Computational aerodynamic modeling for flight dynamics simulation of ram-air parachutes, Aerospace Science and Technology, 54 (2016) 286-301.

[4] C. Dek, J-L. Overkamp, A. Toeter, et al. A recovery system for the key components of the first stage of a heavy launch vehicle, Aerospace Science and Technology, 100 (2020) 105778.

[5] W. Garrard, T. Tezduyar, S. Aliabadi, V. Kalro, J. Luker, S. Mittal, Inflation analysis of ram air inflated gliding parachutes, AIAA Paper 95-1565-CP, 1995.

[6] G.G. Li, Z.C. Deng, Simulation of Parafoil Opening, Journal of National University of Defense Technology, 1993, (4): 16-22 (in Chinese).

[7] J. Potvin, G. Peek, Three-Stage Model for Slider-Reefed Parafoil Inflation, 19th AIAA Aerodynamic Decelerator Systems Technology Conference and Seminar, 2007.

[8] J. Potvin, Momentum-Impulse Balance and Parachute Inflation: Disreefing, Journal of Aircraft, 44 (2007) 691-694.

[9] J. Potvin, G. Peek, B. Brocato, Modeling the Inflation of Ram-Air Parachutes Reefed with Sliders, Journal of Aircraft, 38 (2001) 818-827.

[10] X. Y. Hou, J. Hu, Y. Yu, Numerical study on ring slot parachute finite mass inflation process and wake recontact phenomenon, Aerospace Science and Technology, 128 (2022) 107763.

[11] S.Y. Zhang, L. Yu, Z.H. Wu, H. Jia, X. Liu, Numerical investigation of ram-air parachutes inflation with fluid-structure interaction method in wind environments, Aerospace Science and Technology, 109 (2021) 106400.

[12] China Space News. http://www.spacechina.com/n25/n2018089/n2530233/c2866936/content.html, 2022 (accessed 22 August 2022, in Chinese).
[13] X.Y. Zhang, H.S. Teng, Y. Sui, Z. Wu. Overview of parachute hot air balloon airdrop test technology. Proceedings of the second National Academic Conference on entry, deceleration and landing (EDL) technology. Nanjing, China: 2014. 1-6 (in Chinese).
[14] J.E. Benton, O.A. Yakimenko, On Development of Autonomous HAHO Parafoil System for Targeted Payload Return, AIAA Paper 2013-1312, 2013.
[15] J. McGrath, T. Strong, R. Benney, Status of the Development of an Autonomously Guided Precision Cargo Aerial Delivery System, AIAA Paper 2005-1625, 2005.
[16] J. C. Berland, S. Dunker, S. George, J. Barber, Development of a Low Cost 10,000 lb Capacity Ram-Air Parachute, AIAA Paper 2005-1626, 2005
[17] J. Potvin, R. Montanez, G. Peek, J. Potvin, R. Montanez, G. Peek, The Parks College Ram-Air Parachute Deployment Study: A status report, AIAA Paper 97-1426, 1997
[18] J. Smith, T. Bennett, R. Fox, Development of the NASA X-38 parafoil landing system, AIAA Paper 99-1739, 1999.
[19] J. Stein, C. Madsen, A. Strahan, An Overview of the Guided Parafoil System Derived from X-38 Experience, AIAA Paper 2005-1652, 2005
[20] Z. Zhang, Controllable Recovery of rocket booster using Large-scale Parafoil System for the first time in the world. Spacecraft Recovery & Remote Sensing 2021; 42(4): cover 2 (in Chinese).
[21] Y. Zeng, R. Jiang, H. Liu, B. Chen, W. Hu, Rapid Analysis Method of Parachute Opening Load Base on Acceleration and Attitude Parameters, Structure & Environment Engineering, 48 (2021) 35-39.
[22] W.B. Walcott, Study of Parachute Scale Effects. Report No. AD0296915, 1963.
[23] R.L. Barton, Scale factors for parachute opening: National Aeronautics and Space Administration, NASA technical note: NASA TN D-4123, 1967.
[24] K.E. French, Model law for parachute opening shock, AIAA Journal, 2 (1964) 2226-2228.
[25] J. Lingard, A semi-empirical theory to predict the load-time history of an inflating parachute, AIAA Paper 84-0814, 1984.
[26] C.K. Lee, Modeling of parachute opening - An experimental investigation, Journal of Aircraft, 26 (1989) 444-451.
[27] J. Potvin, Matching the Physics or the Peak Load? Simple Rules for Parachute Inflation Testing at the Full- and Sub-Scales, AIAA Paper 2022-2703, 2022.
[28] H.G. Heinkich, T.R. Hertner, Flexibility as a Model Parachute Performance Parameter, Journal of Aircraft, 8 (1971) 704-709.
[29] E.E. Niemi, P. Bevillard, Modification of Parachute Canopy Stiffness Scaling Laws for Opening Time Prediction, Journal of Aircraft, 52 (2015) 708-713.
[30] E.E. Niemi, R. Gowda, Modification of Parachute Canopy Stiffness Scaling Laws and Application to Tented Structures, AIAA Paper 2013-1382, 2013.
[31] J. Potvin, Testing a new model of ram-air parachute inflation, The Aeronautical Journal, 101 (1997) 299-314.
[32] J. Potvin, More scaling laws for ram-air parachute inflation, AIAA Paper 2001-2072, 2001.
[33] J. Potvin, Altitude- and Weight-Scaling Laws for Ram-Air Parachute Inflation, Journal of Aircraft, 38 (2001) 956-958.
[34] J. Potvin, Universality Considerations for Graphing Parachute Opening Shock Factor Versus Mass Ratio, Journal of Aircraft, 44 (2007) 528-538.
[35] J. Potvin, General Mass Capture Model for Swiftly Opening Parachutes, Journal of Aircraft, 45 (2008) 1689-1700.
[36] M. Budinger, A. Reysset, A. Ochotorena, S. Delbecq, Scaling laws and similarity models for the preliminary design of multirotor drones, Aerospace Science and Technology, 98 (2020) 105658.
[37] L.F. Wang, W.L. He, S.C.Wang, Effects of canopy’s air permeability on parafoil aerodynamic performance. J. Beijing

Univ. Aeronaut. Astronaut, 2017, 43(10): 2021-2029 (in Chinese).
[38] S.Y. Zhang, L. Yu, H. Jia, X.S. Zhao, Similarity criteria for canopy porosity and environmental impact analysis of air permeability, Journal of Industrial Textiles, 51 (2022) 7820s-7834s.
[39] H. Johari, K.J. Desabrais, Stiffness Scaling for Solid-Cloth Parachutes, Journal of Aircraft, 40 (2003) 631-638.
[40] R. Berndt, J. Deweese, Filling Time Prediction Approach for Solid Cloth Type Parachute Canopies, AIAA Paper 1966-1503, 1966.
[41] D. Wolf, Parachute opening shock, AIAA Paper 99-1702, 1999.
[42] J. Potvin, E. Ray, Opening Shock Factor Calculation for Orion Main Parachute Disreefing, AIAA Paper 2019-3486, 2019.
[43] D. Jorgensen, M. Hickey, The AGAS 2000 Precision Airdrop System, AIAA Paper 2005-7072, 2005.
[44] S. Patel, N. Hackett, D. Jorgensen, S. Patel, N. Hackett, D. Jorgensen, Qualification of the Guided Parafoil Air Delivery System-Light (GPADS-Light), AIAA Paper 97-1493, 1997.
[45] J. Potvin, G. Peek, Testing Without Load Cells-Can Opening Shock Be Estimated From Video Data Only?, AIAA Paper 2007-2551, 2007.
[46] M. Cui, K. Yang, X. L. Xu, S. D. Wang, X. W. Gao, A modified Levenberg–Marquardt algorithm for simultaneous estimation of multi-parameters of boundary heat flux by solving transient nonlinear inverse heat conduction problems, International Journal of Heat and Mass Transfer, 97 (2016) 908-916.
[47] D.W. Marquardt, An algorithm for least-squares estimation of nonlinear parameters, Journal of the society for Industrial and Applied Mathematics, 11 (1963) 431-441.